Materials Science in Semiconductor Processing 27 (2014) 343–351

Contents lists available at ScienceDirect

Materials Science in Semiconductor Processing

journal homepage: www.elsevier.com/locate/mssp

Residual strain and electrical resistivity dependence of molybdenum films on DC plasma magnetron sputtering conditions

Majid Khan [a,*], Mohammad Islam [b,c], Aftab Akram [c], Zeming Qi [a], Liangbin Li [a]

[a] National Synchrotron Radiation Laboratory and School of Nuclear Science and Technology, CAS Key Laboratory of Soft Matter Chemistry, University of Science and Technology of China, Hefei 230029, China
[b] College of Engineering, King Saud University, P.O. Box 800, Riyadh 11421, Saudi Arabia
[c] School of Chemical and Materials Engineering, National University of Sciences and Technology, Islamabad 44000, Pakistan

ARTICLE INFO

Keywords:
Molybdenum films
DC-magnetron sputtering
Back contact
X-ray diffraction
Electrical resistivity

ABSTRACT

Sputter deposited molybdenum (Mo) thin films are used as back contact layer for Cu $(In_{1-x}Ga_x)(Se_{1-y}S_y)_2$ based thin film solar cells. Desirable properties of Mo films include chemical and mechanical inertness during the deposition process, high conductivity, appropriate thermal expansion coefficient with contact layers and a low contact resistance with the absorber layer. Mo films were deposited over soda-lime glass substrates using DC-plasma magnetron sputtering technique. A 2^3 full factorial design was made to investigate the effect of applied power, chamber pressure, and substrate temperature on structural, morphological, and electrical properties of the films. All the films were of submicron thickness with growth rates in the range of 34–82 nm/min and either voided columnar or dense growth morphology. Atomic force microscope studies revealed very smooth surface topography with average surface roughness values of upto 17 nm. X-ray diffraction studies indicated, all the films to be monocrystalline with (001) orientation and crystallite size in the range of 4.6–21 nm. The films exhibited varying degrees of compressive or tensile residual stresses when produced at low or high chamber pressure. Low pressure synthesis resulted in film buckling and cracking due to poor interfacial strength as characterized by failure during the tape test. Measurement of electrical resistivity for all the films yielded a minimum $_v$alue of 42 μΩ cm for Mo films deposited at 200 W DC power.

1. Introduction

Thin films of molybdenum (Mo) play an important role as back contact electrode in chalcopyrite (copper–indium–gallium-sulfide–selenide, CIGSSe) and chalcogenide (copper–zinc–tin-sulfide–selenide, CZTSSe) based thin film solar cells [1–5]. Among various metallic films explored as potential back contact layer, Mo and tungsten were found to offer better solar cell efficiencies [6]. Sputter deposited Mo thin films are almost exclusively used in fabrication of chalcogenide (copper–indium-selenide (CIS), copper–indium–gallium diselenide (CIGS)) based thin film solar cells due to (i) chemical inertness during deposition of semiconductor absorber layer, (ii) formation of an ohmic contact, (iii) low recombination rate for minority carriers, (iv) stability at processing temperatures, (iv) low contact resistance, and (iv) resistance to alloying with Cu and In.

It is an established fact that although Mo films with compressive residual stresses exhibit very low sheet

* Corresponding author.
E-mail addresses: majid@mail.ustc.edu.cn, majids@hotmail.com (M. Khan).

http://dx.doi.org/10.1016/j.mssp.2014.07.017
1369-8001/

resistance, their adhesion to the underlying glass substrate is very poor. On the other hand, films containing tensile stresses adhere well to the substrate, yet the electrical resistivity increases by an order. A study on the effect of chamber pressure, residual stresses and sheet resistance of Mo films reported that less than 2 mTorr and in excess of 20 mTorr produced films with compressive residual stresses [7]. Using RF-plasma magnetron sputtering technique, an increase in applied power from 100 to 250 W was found to drastically decrease film resistivity, beside a drop in film growth rate [8]. A low value of electrical resistivity in Mo films is also important to ensure formation of ohmic contact between Mo back electrode and the p-type semiconductor absorber layer [9].

In order to produce Mo back contact electrodes with good adhesion to glass substrate and low electrical resistivity, a bilayer configuration with an initial layer containing tensile residual stresses due to deposition at high pressure followed by a top layer under compression obtained at low chamber pressure. Besides adhesion to the substrate and electrical resistivity, Mo sputter deposition conditions also play an important role in controlling sodium content into the absorber layer that diffuses through it from the glass substrate underneath into the absorber layer over it [5]. A recent study has revealed that increasing the argon pressure during Mo film deposition increases the width of the amorphous oxidized phase (molybdenum trioxide (MoO_3)) inter-grain regions that act as channels for sodium diffusion into the absorber layer [10]. It is noteworthy that voids [11], crystallographic imperfections [12], and argon or oxygen impurities [13,14] in Mo films are some of the causes of residual stresses in sputtered thin films. Also, stress gradients have been reported to develop in Mo thin films as a function of film thickness [15]. The grain size and the magnitude of tensile stresses have been found to increase with an associated decrease in the surface smoothness in case of heavy inert gas atoms in the plasma discharge [16].

In this paper, we present work on Mo thin films deposited under different sets of processing conditions. A design of experiment approach was adopted by defining a 2^3 full factorial design which involves two levels each for applied DC power (P), chamber pressure (p), and substrate temperature (T_s). The design matrix was randomized to minimize systematic error. The effects of process parameters on crystallite size, average surface roughness, residual stresses, and electrical resistivity were assessed to determine what factors and interactions significantly influenced film characteristics.

2. Materials and methods

Small coupons, $10 \times 10 \times 1$ mm^3 in size, were obtained from soda-lime glass slides (Cat. no. 7105) using a diamond saw cutter. First, the substrates were immersed in methanol and cleaned ultrasonically for 20 min in order to remove organic residues. Washing with soap solution was then carried out, followed by rinsing in deionized water. After that, the substrates were immersed in a chromic acid solution for 10 min. Finally, ultrasonic cleaning of the substrates was done in water for 30 min. Following that, the substrate surface was dried by blowing pressurized inert gas and immediately transferred to the deposition chamber.

Deposition of Mo thin films over SLG substrates was done using a disk-shaped Mo target (75 mm diameter, 6.25 mm thickness) in a magnetron sputtering system (Alliance Concept, DP650). The system consisted of mechanical and turbomolecular pumps, six sputtering guns, DC and RF power supplies, and heating and bias capabilities for substrate support. Each film deposition cycle included the following steps: After loading the substrates, the chamber was evacuated to a base pressure of few microTorr, followed by introduction of argon gas. The argon flow rate was maintained at 2 or 18 sccm to achieve respective pressure levels of 1.50 or 9.23 mTorr. The DC-power was then turned on with its value adjusted to the desirable level. Initially, the target was sputtered with its shutter closed for about 15 min to remove any native oxide layer present on its surface. After that, Mo film deposition was carried out to produce films having a thickness of $\sim$1 μm. During growth, the film thickness was monitored by means of a quartz crystal microbalance.

The effect of processing parameters, namely applied power (P), chamber pressure (p), and substrate temperature (T_s) was assessed on resulting film properties, as indicated by the factors and their respective levels in Table 1. Processing conditions, both in coded and uncoded forms, and the sample IDs are listed in Table 1.

The surface morphology and cross-sectional study of Mo thin films were examined using Scanning Electron Microscope SEM (JEOL; JSM 6460) with operating voltage of 15–20 kV, spot size of 30–50 nm and a working distance of 10 mm. The topographical images and average surface roughness values for thin films were obtained from AFM (JEOL SPM 5200) while operating in non-contact mode with scan sizes of 10×10 and 3×3 μm^2. The phase analysis and crystallite size measurement were performed using X-ray diffractometer (STOE; Stadi MP) with Cu-kα radiation ($\lambda = 1.5405$ Å). The values of 2θ range, step size, and dwell time were chosen to be 20–70°, 0.04°, and 3 s, respectively.

Table 1
Sample identification scheme with uncoded and coded parameters listing processing parameters as input variables with their respective levels.

Factor		DC power (P)/W	Pressure (p)/mTorr	Temp. (T)/K			
Level 1 (minimum)		100	1.50	298			
Level 2 (maximum)		200	9.23	673			
Sample ID	Run	Uncoded values			Coded values		
		P (W)	p (mTorr)	T (K)	P	p	T
Mo-0	5	100	1.50	298	0	0	0
Mo-1	6	100	1.50	673	0	0	1
Mo-2	1	100	9.23	298	0	1	0
Mo-3	2	100	9.23	673	0	1	1
Mo-4	7	200	1.50	298	1	0	0
Mo-5	8	200	1.50	673	1	0	1
Mo-6	3	200	9.23	298	1	1	0
Mo-7	4	200	9.23	673	1	1	1

Electrical resistivity values were measured using Hall Effect Measurement System (Ecopia HMS5000). The sheet resistance was determined by Four Point Probe method and then the resistivity was measured. The scotch tape test was performed to determine the adhesion of the film to the substrate. Adhesive tape of the same length was first applied to the film surface and then removed manually with approximately the same force for all the samples. The quality of interfacial adhesion between the film and the underlying substrate was investigated by examining the sample surface under light optical microscope (Sinowon, UMS-300).

3. Results and discussion

3.1. Structural and compositional analysis

The effect of P on film surface morphology was assessed by examining samples Mo-2 and Mo-6 that were prepared at the same p and T_s values of 9.2 mTorr and 298 K, respectively. High magnification SEM images of the film surfaces revealed strikingly different topographies, as shown in Fig. 1. While the film produced at 100 W indicated the presence of surface features, those obtained from high power deposition were much smoother. It is possible that the relatively higher energy of the incident species caused an enhanced degree of surface diffusion in the growing film [17]. Also, an increase in applied power was found to almost double the film growth rate, as determined using quartz crystal microbalance.

For better resolution and average surface roughness (R_a) measurement, the films were examined under atomic force microscope (AFM), as presented in Fig. 2. The observations made were in accordance with the literature where film deposition at high pressure was reported to produce a surface structure consisting of round, bumpy grains [2]. The effect of P while maintaining high p and T_s values can be investigated in samples Mo-3 and Mo-7. Two- and three-dimensional surface microstructures with AFM scan size of 3 μm, shown in Fig. 3(g and h), revealed the presence of coarse grains when deposition was carried out at 200 W and 673 K. Comparison of samples Mo-2 and Mo-3 revealed that higher T_s value leads to enhanced surface mobility of the deposited species and a resultant decrease in R_a value, as manifested by the z-axis limit in Fig. 2(b and d). The same parameter, i.e. T_s did not have a significant effect in case of Mo-6 and Mo-7 deposited at 200 W. The average surface roughness (R_a) values for most of the samples are listed in Table 2.

Film thickness and growth morphology were determined from examination of film cross-sections, shown in Fig. 3. Low magnification SEM images indicated thickness uniformity over large substrate area and high magnification revealed film morphology during growth. All the films examined were sub-micron thick with the corresponding growth rate in the range of ~37–78 nm/min depending on processing conditions. It was noticed that the deposition rate almost doubled upon increasing the applied power to 200 W. This is understandable since sputter yield strongly depends on applied power. Similar trends were reported for nickel, alumina and silicon dioxide films produced using RF-plasma magnetron sputtering technique [18,19]. Film deposition at high T_s resulted in dense structure and greater film thickness as manifested in the case of samples Mo-2 (Fig. 3d) and Mo-3 (Fig. 3f), whereas voided, columnar structure produced as a result of oblique flux of the incident species was seen in case of room temperature growth. With other processing parameters being the same, higher T_s of 673 K (Mo-2 versus Mo-3) produced dense films with more thickness due to the greater extent of incorporation of incident species through surface and volumetric diffusion. The cross-section of sample Mo-4 (Fig. 3g and h) revealed delamination from the substrate that might have occurred during the sample preparation stage. Films prepared under such processing conditions exhibited high compressive residual stresses as demonstrated by failure during the tape test (discussed later).

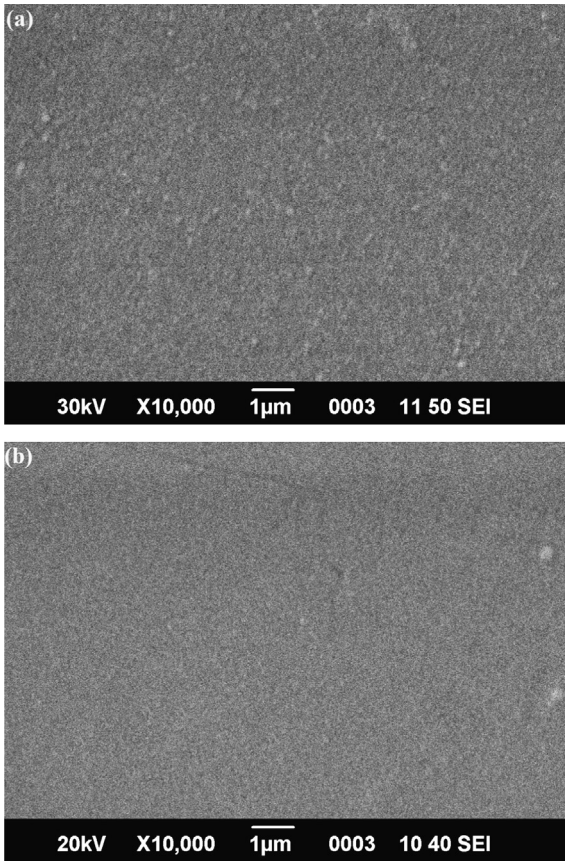

Fig. 1. SEM microstructures of the Mo films deposited at the same pressure and temperature (1, 0) but different values of applied power (a) 0 and (b) 1. [0 (min) and 1 (max) are coded values].

X-ray diffraction spectra were obtained for most of the samples, as shown in Fig. 4. Any shift in the actual position of a crystallographic peak may be indicative of the internal residual stresses in the films that originate due to several factors such as voids, crystal defects, and/or incorporation of oxygen and argon in the films [3], causing issues related to adhesion and long-term reliability. The nature and intensity of residual stress is a function of change in lattice constant with respect to that of the undeformed lattice (0.3147 nm for Mo), and can be expressed mathematically

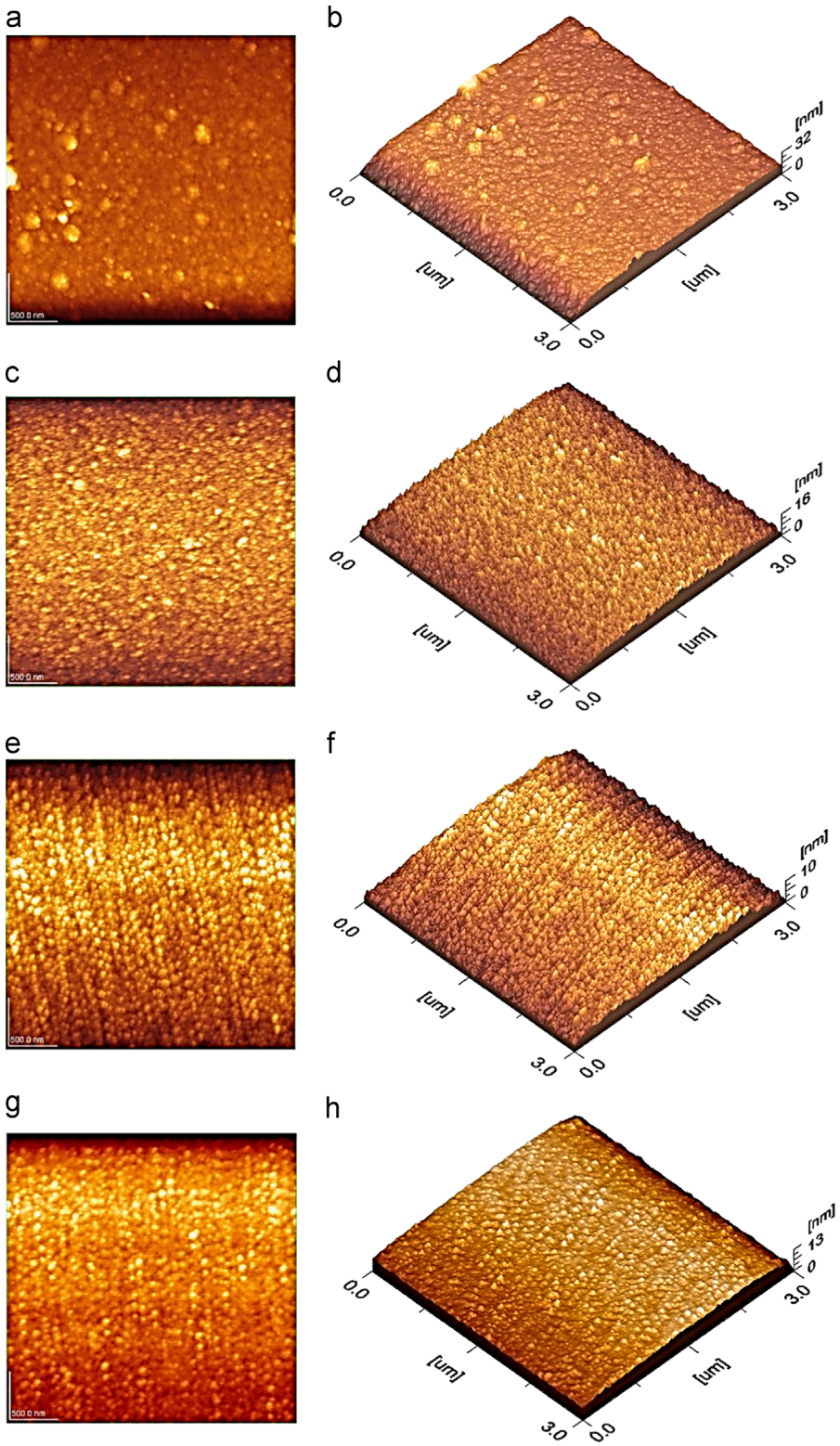

Fig. 2. Two- and three-dimensional topographical representations of the Mo thin films (Table 2): (a, b) Mo-2, (c, d) Mo-3, (e, f) Mo-6, and (g, h) Mo-7.

as strain (%)$=\Delta a/a_o$ (%). The crystallite size was calculated using Scherer's formula, $t=0.9\kappa\lambda/(\beta\cos\theta)$, where κ, λ, β, and θ are the respective values of Scherer constant (0.94), the wavelength of incident radiation (1.5405 for Cu-kα), full-width at half-maximum (FWHM), and diffraction angle. In all cases, single peaks with different relative intensities

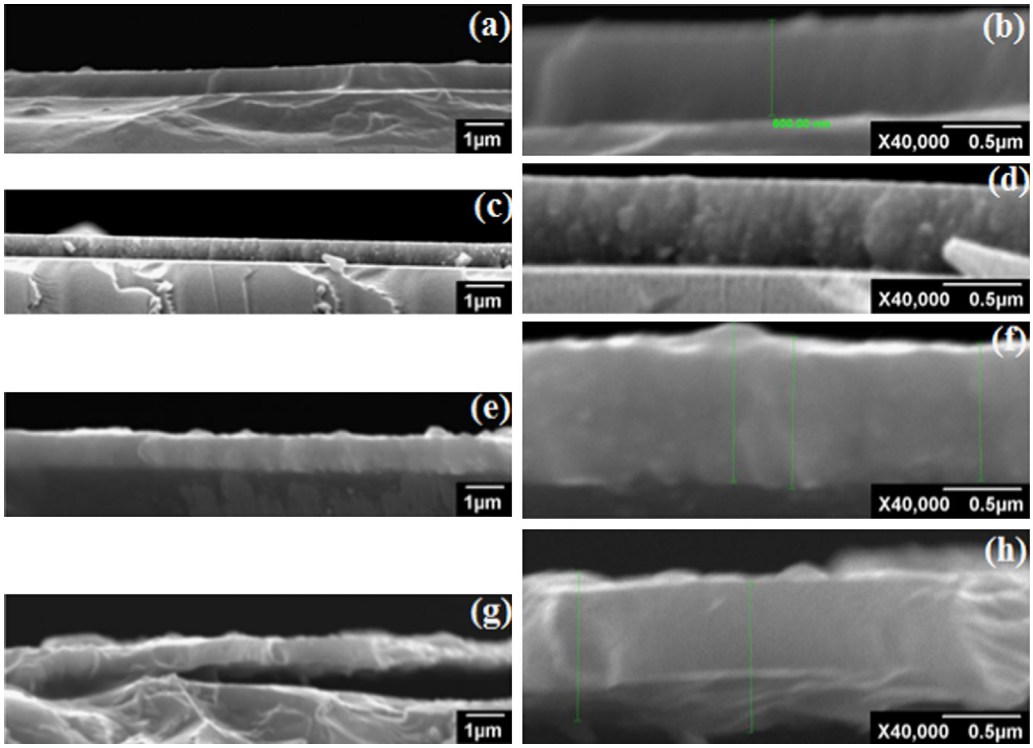

Fig. 3. Low and high magnification microstructures of the Mo film cross-sections (Table 2): (a, b) Mo-1, (c, d) Mo-2, (e, f) Mo-3, and (g, h) Mo-4.

Table 2
Different properties of Mo films as determined using different characterization techniques.

Sample ID	Thickness (nm)	Rate (nm min^{-1})	Surface roughness (nm)	Crystallite size (nm)	Strain (%)	Resistivity (μΩ cm)	Tape test
Mo-0	515	34.3		4.4	−1.40	202	Fail
Mo-1	586	39.1			−1.02	180	Fail
Mo-2	530	37.9	6.3		0.68	257	Pass
Mo-3	892	63.7	9.5	9.4	2.32	274	Pass
Mo-4	625	78.1	10.6	15.9	−0.84	44.3	Fail
Mo-5	610	82.4			−1.03	42.7	Fail
Mo-6	545	68.1	7.5	21.5	0.56	140	Pass
Mo-7	574	76.5	5.4	20.6	0.73	98.7	Pass

were observed. The crystal structure was indexed to be cubic (JCPDS card no. 3-065-7442) with (110) orientation. Using full width at half maximum (FWHM) value for each film, the crystallite size was calculated to be in the range of ~4.4–21.5 nm, depending on deposition conditions. The crystallite size was found to increase upon increasing either chamber pressure or DC-power with maximum size determined for films deposited at 200 W and 9.23 mTorr. Applied power, chamber pressure and substrate temperature (to a lesser extent) promote surface diffusion of the arriving species with resultant increase in crystalline quality and crystallite size that is manifested by an increase in peak intensity and an associated decrease in FWHM value. The findings are in agreement with the earlier work that assessed the effect of power, pressure, and substrate temperature on mechanical and electrical properties of the Mo films [2,8,20,21]. The values of crystallite size and residual stress in the Mo films, calculated from XRD data, are listed in Table 2.

3.2. Residual stresses and adhesion

Results from tape tests performed on Mo films indicated that films deposited at low pressure of 1.50 mTorr, i.e. Mo-0, Mo-1, Mo-4, and Mo-5, failed by exhibiting varying degrees of interfacial delamination. Mo films grown at relatively high pressure of 9.23 mTorr (Mo-2, Mo-3, Mo-6, Mo-7) remained firmly adhered to the underlying glass substrate. Micrographs of some of the Mo films after the tape test as obtained after examination under light optical microscope are presented in Fig. 5. From the micrographs recorded at 400× magnification, the dark regions represent areas from where the film was removed as a result of tape test, whereas light spots indicate the

presence of the film over glass substrate. From comparison of Mo-0 and Mo-1 films, it is evident that the sample Mo-0 readily failed as exhibited by much greater degree of film delamination. It is speculated that the magnitude of residual compressive stresses was higher in the case of Mo-0 film than those present in the Mo-1 film. Since Mo-1 was produced at high T_s, it is believed that high temperature during film growth promoted rearrangement and densification of deposited species, thus leading to a less degree of residual stress incorporation. The other two samples, Mo-3 and Mo-7, did not undergo any film delamination during the tape test as evident from Fig. 5(c and d).

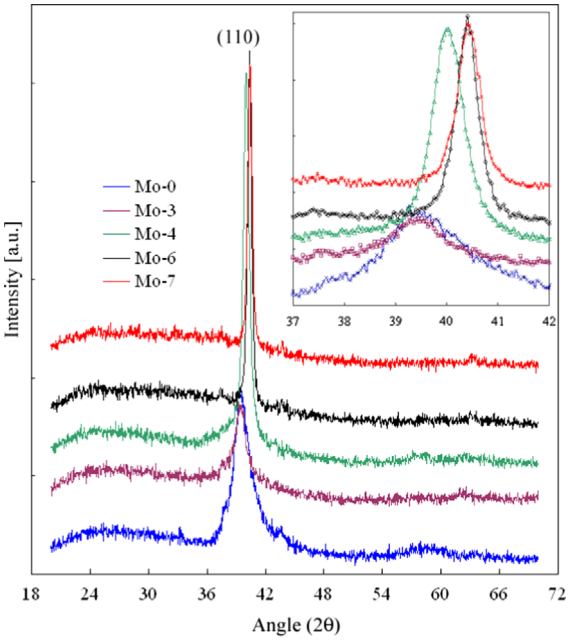

Fig. 4. X-ray diffraction spectra of different Mo thin films with the inset showing the precise position of the (110) peak.

SEM examination of the films deposited at low chamber pressure (1.50 mTorr) suggested buckling of the films, which in extreme cases, led to film cracking or tearing. Comparison of the samples Mo-0 and Mo-4, which were prepared under similar p and T_s conditions, at different applied powers, revealed different degrees of compressive residual stresses, as evident from surface microstructures, as shown in Fig. 6(a and b). Although the degree of waviness exhibited by sample Mo-0 was much less than that of Mo-4, very long cracks with lengths of the order of hundreds of microns were seen. Film growth at high P and T_s as in the case of sample Mo-5 was found to induce a large degree of compressive stresses that led to extensive film cracking and delamination. This behavior may be attributed to mismatch in coefficient of thermal expansion between the film and the underlying substrate. From tape tests and microstructural examination, it can be qualitatively deduced that the samples Mo-0 and Mo-5 (low chamber pressure deposition) possess a higher degree of

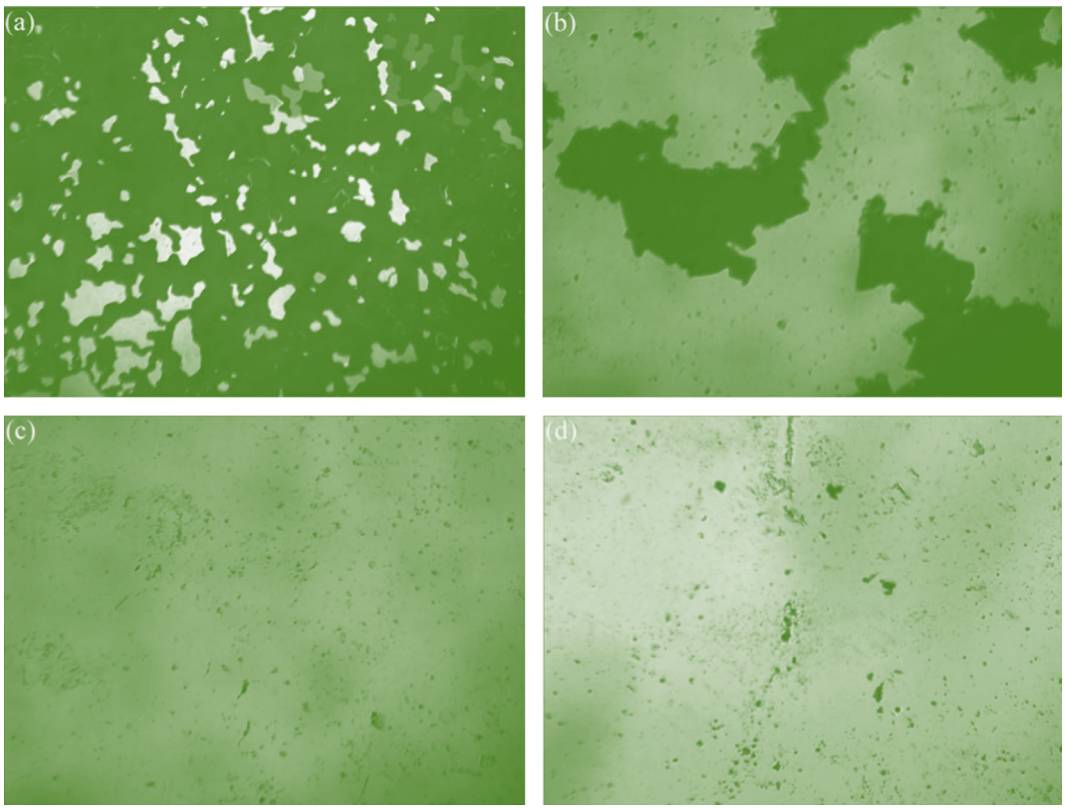

Fig. 5. Surface microstructures of the films (Table 2) after tape test: (a) Mo-0, (b) Mo-1, (c) Mo-3, and (d) Mo-7. The magnification is 400 × . i.e. a length of 1 cm represents 25 μm.

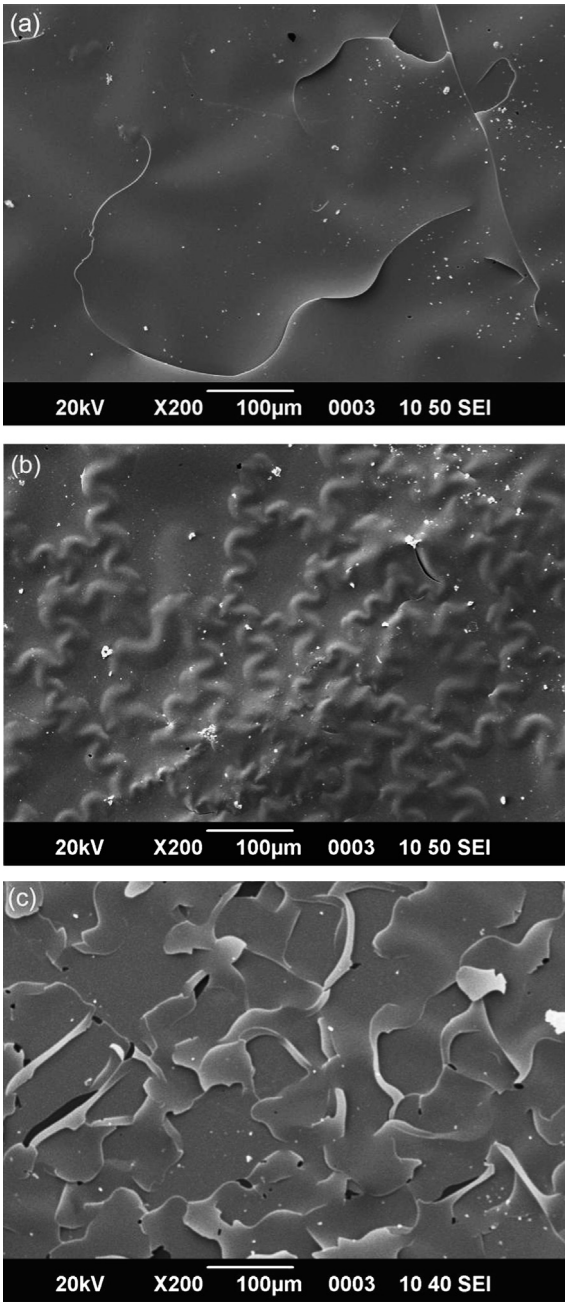

Fig. 6. Low magnification SEM images of the Mo film surfaces obtained from different processing conditions (Table 2): (a) Mo-0, (b) Mo-4, and (c) Mo-5.

compressive stresses than samples Mo-1 and Mo-7 (high T_s growth), irrespective of the applied DC power.

3.3. Electrical resistivity of Mo films

Depending on the film growth conditions, the electrical resistivity was found to have values in the range of 42–275 μΩ cm. The resistivity values for both samples Mo-4 and Mo-5 were much lower than the other samples, although it is believed that further reduction in electrical resistivity can be achieved through fine tuning of film growth conditions. The fact that films with residual compressive stresses exhibited minimum electrical resistivity is in accordance with the published literature [7,22]. Comparison of electrical properties based on film growth conditions revealed that the substrate temperature did not have a significant effect on resistivity values, whereas Mo films deposited at 200 W DC power always had lower electrical resistivity values than their counterparts produced at 100 W. Similarly, films deposited at low chamber pressure (1.50 mTorr) were determined to have low electrical resistivity than those produced at high pressure (9.23 mTorr).

3.4. Assessment of significant factors and their mutual interactions

The effect of an individual input parameter, also known as the main effect, is computed by taking the difference of the response factor values for high and low values of that factor. Mathematically, the calculation of an effect is expressed as follows:

$$\text{Effect} = \frac{\sum Y_1}{n_1} - \frac{\sum Y_0}{n_0} \quad (1)$$

where the "n"s refer to the number of data points collected at each level. The "Y"s referred to the associated responses.

For the three main factors (P, p and T), the graphs of mean values of electrical resistivity against low and high level of each main effect are presented in Fig. 7a. Among all the three main factors, power (P) and pressure (p) have a significant effect on the electrical resistivity of the Mo films. The negative slope of the graph in case of power, however, indicates that increasing the applied DC power causes a drop in electrical resistivity. Thus, lower resistivity values can be obtained through Mo film deposition at high DC power and low chamber pressure.

Investigation into the effect of processing conditions on percent strain in the films reveal chamber pressure to be the only significant main effect, as indicated in Fig. 7b. In both cases, the substrate temperature is not found to significantly influence Mo film resistivity and percent strain values.

To examine individual and cumulative effect of the main factors and their mutual interactions, Pareto charts were plotted. In a Pareto chart, all the factors and their mutual interactions are arranged as bars with their magnitudes in descending order. For a confidence level of 90% (α=0.10), the Pareto charts of effects were produced with resistivity and percent strain as response variables, as shown in Fig. 8. The findings confirm power and pressure to be the significant main factors with power having more significant contribution than chamber pressure. Also, no interaction between main factors was significant as evident from a Pareto plot of effects with electrical resistivity as response variable (Fig. 8a). On the other hand, when percent strain is the response

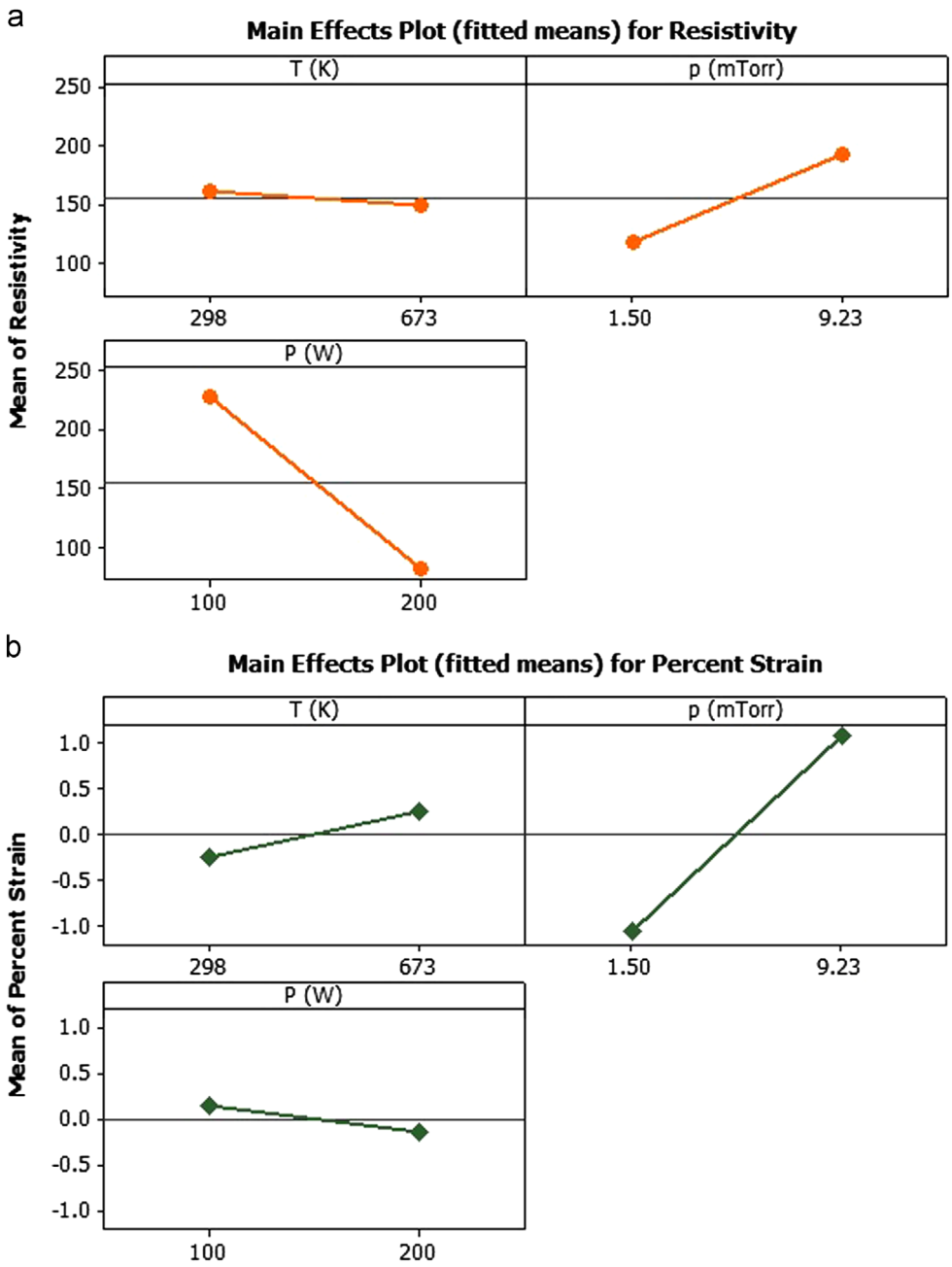

Fig. 7. Main effects plot for substrate temperature (T), pressure (p) and power (P) with different response variables: (a) mean electrical resistivity and (b) percent strain.

variable, chamber pressure (p) is the significant effect among all the main factors, as shown in Fig. 8b. The Pareto chart indicates that for a confidence interval of 90% ($\alpha=0.10$), pressure is the only significant effect. A direct correlation exists between p and % strain which implies that the magnitude of residual stresses will increase upon increasing the chamber pressure. The inferences drawn from statistical analysis are in agreement with the conclusions made in the preceding section.

4. Conclusions

Molybdenum thin films were prepared at different processing conditions, namely, DC power, chamber pressure, and substrate temperature by defining a 2^3 factorial design with two levels of each variable. All the films exhibited preferred orientation along (110) plane with varying deviations from peak position, peak intensity, and FWHM values. Films prepared at low pressure of 1.50 mTorr were found to be under compressive residual stress and failed during the

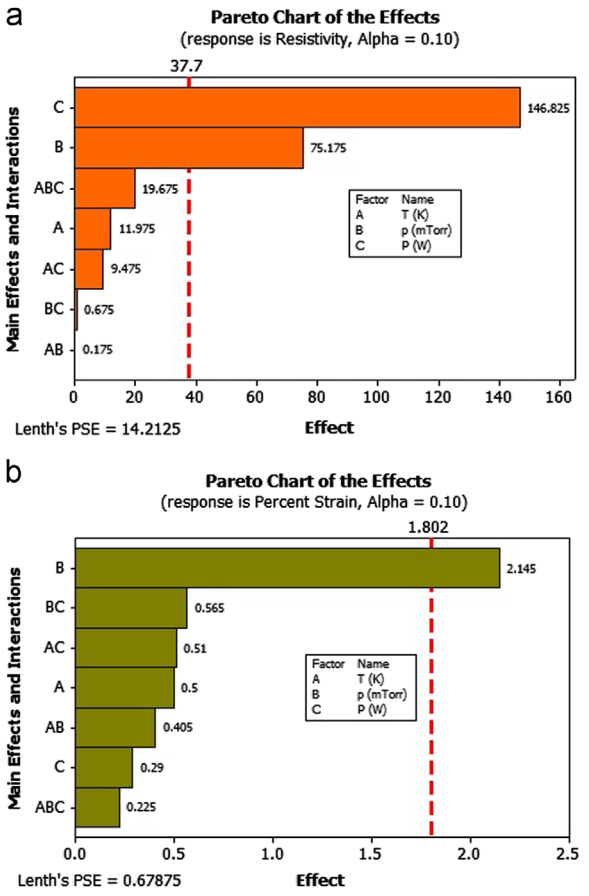

Fig. 8. Pareto chart of effects (α=0.10) for response variables of (a) electrical resistivity and (b) percent strain.

tape test. Increasing the applied DC power resulted in relatively higher crystallite size in the deposited films.

Minimum electrical resistivity values were determined for films obtained at high power (200 W) and low pressure (1.50 mTorr) presumably due to surface and volumetric diffusion during film growth that induced dense morphology. Strongly adherent films with slightly higher resistivity were produced at high power (200 W) and pressure (9.23 mTorr). Films prepared at high power (200 W) and substrate temperature (673 K) offer near optimal attributes that can be further improved through fine tuning of processing conditions.

Main effects' plots and Pareto chart indicated applied power and chamber pressure to be significant factors that influence electrical resistivity of the Mo thin films. On the other hand, when percent residual stress was considered as the response variable, chamber pressure during film growth was found to be the main significant variable.

Acknowledgments

The authors would like to thank the Higher Education Commission, Pakistan for funding this research through its National Research Program for Universities (Grant no. 20-1603).

References

[1] Z.H. Li, E.S. Cho, S.J. Kwon, Appl. Surf. Sci. 257 (2011) 9682–9688.
[2] M.A. Martinez, C. Guillen, Surf. Coat. Technol. 110 (1998) 62–67.
[3] T.K. Todorov, K.B. Reuter, D.B. Mitzi, Adv. Mater. 22 (2010) E156–E159.
[4] H. Katagiri, K. Jimbo, S. Yamada, T. Kamimura, W.S. Maw, T. Fukano, T. Ito, T. Motohiro, Appl. Phys. Express 1 (2008) 041201.
[5] H.A. Al-Thani, F.S. Hasoon, M. Young, S. Asher, J.L. Alleman, M.M. Al-Jassim, D.L. Williamson, Proceedings of 29th IEEE PV Specialists Conference, New Orleans, Louisiana (2002).
[6] K. Orgassa, H.W. Schock, J.H. Werner, Thin Solid Films 387 (2003) 431–432.
[7] J.H. Scofield, A. Duda, D. Albin, B.L. Ballard, P.K. Predecki, Thin Solid Films 260 (1995) 26–31.
[8] Y.W. Yen, Y.L. Kuo, J.Y. Chen, C. Lee, C.Y. Lee, Thin Solid Films 515 (2007) 7209–7216.
[9] G. Gordillo, F. Mesa, C. Calderon, Braz. J. Phys. 36 (2006) 982–985.
[10] E. Gautron, M. Tomassini, L. Arzel, N. Barreau, Surf. Coat. Technol. 211 (2012) 29–32.
[11] T.J. Vink, M.A.J. Somers, J.L.C. Daams, A.G. Dirks, J. Appl. Phys. 70 (1991) 4301.
[12] J.A. Thornton, D.W. Hoffman, Thin Solid Films 171 (1989) 5–31.
[13] T. Yamaguchi, R. Miyagawa, Jpn. J. Appl. Phys. 30 (1991) 2069–2073.
[14] T.T. Bardin, J.G. Pronko, R.C. Budhani, J.S. Lin, R.F. Bunshah, Thin Solid Films 165 (1988) 243–247.
[15] S.G. Malhotra, Z.U. Rek, S.M. Yalisove, J.C. Bilello, J. Vac. Sci. Technol. A 15 (1997) 345–352.
[16] G.T. West, P.J. Kelly, Surf. Coat. Technol. 206 (2011) 1648–1652.
[17] M. Khan, M. Islam, Semiconductors+. 47 (2013) 1610–1615.
[18] M. Islam, O.T. Inal, J.R. Luke, J. Appl. Phys. 100 (2006) 084903.
[19] M. Islam, O.T. Inal, J. Vac. Sci. Technol. A 26 (2008) 198–204.
[20] L. Assmann, J.C. Bernede, A. Drici, C. Amory, E. Halgand, M. Morsli, Appl. Surf. Sci. 246 (2005) 159–166.
[21] M. Khan, M. Islam, A. Akram, U. Manzoor, Surf. Rev. Lett. 6 (2013) 1350065.
[22] S.Y. Kuo, L.B. Chang, M.J. Jeng, W.T. Lin, Y.T. Lu, S.C. Hu, Mater. Res. Soc. Symp. Proc. 1123 (2009) 05–18.